Available online at www.sciencedirect.com
SCIENCE DIRECT®
Solar Energy xxx (2005) xxx–xxx
SOLAR ENERGY
www.elsevier.com/locate/solener

Solar water splitting for hydrogen production with monolithic reactors

C. Agrafiotis [a], M. Roeb [b], A.G. Konstandopoulos [a,*], L. Nalbandian [a], V.T. Zaspalis [a], C. Sattler [b], P. Stobbe [c], A.M. Steele [d]

[a] *Chemical Process Engineering Research Institute, Center for Research and Technology—Hellas (CERTH/CPERI), P.O. Box 361, 57001 Thermi-Thessaloniki, Greece*
[b] *Deutsches Zentrum für Luft- und Raumfahrt e.V. (DLR), Institut für Technische Thermodynamik, Solarforschung, D-51170 Köln, Germany*
[c] *Stobbe Tech Ceramics (STC), Vejlemosevej 60, DK-2840, Holte, Denmark*
[d] *Johnson Matthey Fuel Cells Centre, Sonning Common, RG4 9NH Reading, UK*

Received 21 July 2004; received in revised form 12 November 2004; accepted 23 February 2005

Communicated by: Associate Editor Sixto Malato-Rodríguez

Abstract

The present work proposes the exploitation of solar energy for the dissociation of water and production of hydrogen via an integrated thermo-chemical reactor/receiver system. The basic idea is the use of multi-channelled honeycomb ceramic supports coated with active redox reagent powders, in a configuration similar to that encountered in automobile exhaust catalytic aftertreatment.

Iron-oxide-based redox materials were synthesized, capable to operate under a complete redox cycle: they could take oxygen from water producing pure hydrogen at reasonably low temperatures (800 °C) and could be regenerated at temperatures below 1300 °C. Ceramic honeycombs capable of achieving temperatures in that range when heated by concentrated solar radiation were manufactured and incorporated in a dedicated solar receiver/reactor. The operating conditions of the solar reactor were optimised to achieve adjustable, uniform temperatures up to 1300 °C throughout the honeycomb, making thus feasible the operation of the complete cycle by a single solar energy converter.

Keywords: Water-splitting; Solar; Redox materials; Iron oxide; Honeycomb reactors; Hydrogen

1. Introduction

The harnessing of the huge energy potential of solar radiation and its effective conversion to chemical energy carriers such as hydrogen is a subject of primary technological interest. One of the reactions with tremendous economical impact because of the low value of its reactants is the dissociation of water (water splitting) to

* Corresponding author. Tel.: +30 2310 498192; fax: +30 2310 498190.
E-mail address: agk@cperi.certh.gr (A.G. Konstandopoulos).

0038-092X/$ - see front matter © 2005 Elsevier Ltd. All rights reserved.
doi:10.1016/j.solener.2005.02.026

oxygen and hydrogen. The integration of solar energy concentration systems with systems capable to split water is of immense value and impact on the energetics and economics worldwide; by some is considered as the most important long-term goal in solar fuels production to cut hydrogen costs and ensure virtually zero CO_2 emissions (Rubbia, 2003; Kodama, 2003; Steinfeld, 2005).

The dissociation of water is a reaction not favoured thermodynamically; one has to go up to extremely high temperatures (>2200 °C) for obtaining some significant dissociation degree (Kodama, 2003). Moreover, direct one-step water splitting (thermolysis) requires the energy intensive process of high temperature oxygen–hydrogen separation coupled with expensive membrane technology (Kogan, 2000) and therefore is considered of little chance for technical and economical viability in the near future (Perkins and Weimer, 2004). The current state of the art of solar chemistry for water splitting and hydrogen production is focused on the so-called redox pair cycles. These are two-step processes, based on redox materials that can act as effective water splitters at lower temperatures. According to this idea, in the first step (water-splitting) the activated redox reagent (usually the reduced state of a metal oxide) is oxidized by taking oxygen from water and producing hydrogen, according to the reaction:

$$MO_{red} + H_2O\ (g) \rightarrow MO_{ox} + H_2\ (g) \quad (1)$$

During the second step the oxidized state of the reagent is reduced, to be used again (re-generation), delivering some of the oxygen of its lattice according to the reaction:

$$MO_{ox} \rightarrow MO_{red} + \tfrac{1}{2}O_2 \quad (2)$$

The disadvantage is that a two-step process is required, consisting of a water splitting and a regeneration (oxygen release) step. The advantage is the production of pure hydrogen and the removal of oxygen in separate steps, avoiding the need for high-temperature separation and the chance of explosive mixtures formation.

Current research efforts have focused on thermochemical cycles based on various types of ferrites (Tamaura et al., 1995, 1998a,b, 1999, 2001; Kaneko et al., 2001, 2002a,b; Kojima et al., 1996; Kodama et al., 2003), iron oxide (Weidenkaff et al., 1997; Ehrensberger et al., 1995, 1996), manganese oxide (Sturzenegger and Nuesch, 1999), zinc oxide (Steinfeld, 2002) and combinations of the above (Steinfeld et al., 1998, 1999). It has been suggested that the only feasible two-cycle redox pairs are ZnO/Zn and Fe_3O_4/FeO (Steinfeld et al., 1999). The concept has been proven experimentally: with the most active of these materials, water splitting has reportedly taken place at temperatures as low as 627 °C (Tamaura et al., 1998b; Steinfeld et al., 1999), however the regeneration temperatures are still high (>1300 °C), a most important problem since it can cause significant sintering of the metal oxide. Attempts to tackle this problem have been recently realized by supporting the redox reagent on high-temperature–stable ZrO_2 fine particles (Kodama, 2003; Kodama et al., 2003). In addition, in such systems it is necessary to quench the reduction products (Zn/FeO respectively) in order to avoid reoxidation, a fact introducing irreversibilities and complexities in large-scale utilization (such as separate packed bed reactors for the water splitting and for the regeneration step).

It has been shown though, that complete reduction of an oxide to the respective metal is not necessary: cation excess (oxygen deficient) Ni–Mn spinel ferrites were proven capable for both water splitting and regeneration (Tamaura et al., 1995, 1998b; Kojima et al., 1996). In such systems in the first endothermic step the ferrite ($Ni_{0.5}Mn_{0.5}Fe_2O_4$ for instance in Tamaura et al., 1995) was thermally activated above 800 °C to form an oxygen-deficient ferrite $Ni_{0.5}Mn_{0.5}Fe_2O_{4-\delta}$ (where δ indicates the oxygen deficiency of the spinel); in the second step the activated ferrite reacted with water below 800 °C to form hydrogen and the initial ferrite. It has been reported that partial substitution of iron in the spinel phase by Mn, Ni or Zn, forms mixed metal oxides of the type $(M_xFe_{1-x})_3O_4$ that are more reducible and require moderate, more workable upper operating temperature (Steinfeld et al., 1998). These ferrites can contain not only the dopant metals in the divalent state but a significant portion of iron as well; thus all possible oxidations to the trivalent state can be exploited for oxygen uptake from water. Therefore, such spinel materials are considered as very attractive candidates since one can make use of the percentage of the divalent metal(s) present in the spinel phase and "oscillate" during the redox cycle between the activated and non-activated structure without undergoing phase transformations (such as to the lower-valence metal oxide or to the respective metal). In addition, further enhancement of their water splitting capability is expected if they can be synthesized with a high concentration of oxygen vacancies in their crystal lattices (lattice defects). Stoichiometric defects such as oxygen vacancies and their mobility on the oxide surface are of great importance for redox reactions involving gases and oxides of metals with multiple oxidation states and are widely exploited in oxygen-storage materials, the most common example being CeO_2 used in catalytic gas exhaust aftertreatment (Trovarelli, 1996). The enhanced water splitting activity of non-stoichiometric wustite ($Fe_{1-y}O$) materials has been attributed to the large amount of defect clusters serving as nuclei for magnetite formation (Weidenkaff et al., 1997) and that of ZrO_2-supported $Mn_{0.36}Fe_{2.64}O_4$ in the contribution of oxygen-deficient ZrO_2 phases (Kodama et al., 2003).

Despite basic research with respect to active redox pairs, solar reactor concepts have only recently been re-

ported in the literature. Some (Steinfeld et al., 1999; Steinfeld, 2005; Kaneko et al., 2004; Palumbo et al., 2004) are based on particles fed into rotating cavity reactors, concepts that are complicated and costly to operate. In the present work, an innovative solar water splitting reactor is proposed based on two concepts: the synthesis of active iron-oxide-based redox pairs and their incorporation upon multi-channelled monolithic honeycomb structures capable for achieving and sustaining high temperatures.

Ceramic multi-channelled monolithic honeycomb reactors offer an attractive alternative to packed beds when dealing with gaseous reactants at high temperatures; their advantages include thin walls, high geometric surface area and therefore good gas–solid contact, low pressure drop, good mass transfer performance and ease of product separation (Heck and Farrauto, 1995). Further benefits can be gained from special material properties such as thermal shock resistance and mechanical strength. With respect to exploitation of solar energy in particular, the absorbance of silicon carbide (SiC) coupled with its high thermal conductivity enables the collection of solar heat and effective heating of the reactant gases inside the honeycomb channels. It has already been demonstrated that SiC monoliths can act as collectors of solar heat and achieve temperatures in excess of 1100 °C (Hoffschmidt et al., 2001; Fend et al., 2004). Provided that the redox pairs to be developed are capable for both water splitting and regeneration at these temperature levels, the full cycle can be performed with the redox material immobilized upon the honeycomb walls (Konstandopoulos et al., 2000, 2005) avoiding the needs of continuous powder feeding and collection from the reactor. The proposed concept not only produces hydrogen but employs the use of renewable solar energy without any CO_2 emissions, in an entirely "clean", natural and environmentally friendly way.

2. Experimental

In this work, three routes were employed for the synthesis of iron-oxide-based redox materials: in the first, the mixed oxides were prepared with "conventional" solid-state synthesis via sintering of the respective oxides in a controlled-atmosphere sintering furnace; after the calcination step the materials were cooled under controllable oxygen partial pressure so that materials with controllable defect chemistry were obtained (Tsakaloudi et al., 2004). The second route involved the so-called self-propagating high-temperature synthesis (SHS or combustion synthesis) reactions between iron metal powder and oxygen in the presence of the dopant metal oxides (Agrafiotis and Zaspalis, 2004). The third route selected was Aerosol Spray Pyrolysis where a liquid solution of the metal precursor salts is atomized in a spray of fine droplets and subsequently passed through a high-temperature tube furnace where it transforms within a very short time to the desired powder (Lorentzou et al., 2004). The two latter methods provide an alternative way for synthesis of materials with high defects concentration due to their common characteristic of very short synthesis times and extremely high cooling rates; in addition they can also take place within reactors that can provide for controlled oxygen partial pressure, therefore "tuning" further the products' oxygen vacancies concentration.

Redox material powders synthesized via the methods above were subsequently laboratory-tested with respect to water-splitting activity and regeneration capability in the form of powders as described below. These series of experiments were focussed on determining the most promising material compositions, to be thereafter synthesized in larger quantities and used for the coating of SiC honeycombs for the eventual solar testing. In parallel, the dedicated solar reactor was designed, built and tested in a solar furnace facility, in order to minimise temperature gradients within the volume of the honeycomb absorber and develop the proper solar test programme. A detailed description of the experimental procedure follows.

2.1. Powder synthesis

2.1.1. Solid-state synthesis (SSS)

For the reasons argued above the targeted redox materials were MnZn- or NiZn-doped ferrites crystallized in the spinel structure. They were synthesized by the typical mixed oxide route, which includes powder mixing of component oxides, prefiring, milling, spray drying and calcination at high temperatures (≈1250 °C) according to the scheme (Mn–Zn ferrites):

$$Fe_2O_3 + (x/3)Mn_3O_4 + (1-x)ZnO \rightarrow (Mn_xZn_{1-x})Fe_2O_4 \quad (3)$$

For the synthesis of the respective Ni–Zn ferrites, Mn_3O_4 was replaced by NiO. As already mentioned, during cool down, the Mn–Zn materials were maintained under controlled O_2 partial pressure (following the equilibrium curve of Fe^{+2}/Fe^{+3}) in order to prevent complete oxidation of Fe^{+2} to Fe^{+3}, whereas Ni–Zn ferrites were cooled under air atmosphere.

2.1.2. Self-propagating high-temperature synthesis (SHS)

The same targeted materials were synthesized via combustion reactions between iron metal powder and oxygen in the presence of the dopant metal oxides and of Fe_2O_3 powder as a "thermal ballast/moderator" to control the synthesis temperature, according to the scheme (Agrafiotis and Zaspalis, 2004):

$$2k\mathrm{Fe} + (1-k)\mathrm{Fe_2O_3} + (x/3)\mathrm{Mn_3O_4} + (1-x)\mathrm{ZnO} + (1.5k)\mathrm{O_2} \rightarrow (\mathrm{Mn}_x\mathrm{Zn}_{1-x})\mathrm{Fe_2O_4} \quad (4)$$

Similarly, for the synthesis of the Ni–Zn ferrites, Mn_3O_4 was replaced by NiO. The quantities of the two reactant dopant oxides (ZnO and either Mn_3O_4 or NiO) were calculated so that $x = 1 - x = 0.5$. Temperatures in excess of 1000 °C were achieved, whereas the synthesis times were of the order of few seconds. However, the product was not always of the spinel ferrite phase. The effect of the ratio of reactant Fe powder to Fe_2O_3 "moderator" ($2k/1-k$) and of the oxygen content determines the phase composition of the products. Low values of the (fuel/moderator) ratio ($k = 0.3$) are not sufficient to complete the reaction, "intermediate" values ($k = 0.5$) favour the formation of single-phase spinels $(Mn_{0.5}Zn_{0.5})Fe_2O_4$ whereas a high value ($k = 0.9$) favours the formation of the "least-oxygen-containing" doped wustite ($Mn_xZn_yFe_{1-x-y}O$) as the main phase. Both series of products—spinels and wustites—were checked with respect to water splitting activity.

2.1.3. Aerosol spray pyrolysis (ASP)

Aqueous solutions of nitrates of Fe, Zn, Mn and Ni with the addition of citric acid and ammonia, were atomized in sprays of fine droplets and subsequently passed through a high-temperature tube furnace to be transformed within a short time to the desired powder according to the scheme:

$$2\mathrm{Fe(NO_3)_3} + x\mathrm{Mn(NO_3)_2} + (1-x)\mathrm{Zn(NO_3)_2} + 3\mathrm{C_6O_7H_8} + 8\mathrm{NH_3} + 9.5\mathrm{O_2} \rightarrow (\mathrm{Mn}_x\mathrm{Zn}_{1-x})\mathrm{Fe_2O_4} + 18\mathrm{CO_2} + 8\mathrm{N_2} + 24\mathrm{H_2O} \quad (5)$$

Similarly to the previous methods, either $Mn(NO_3)_2$ or $Ni(NO_3)_2$ was used. The ASP experiments took place in a stainless steel reactor tube, heated between 350 and 1070 °C. Air was used as a carrier gas and the residence time varied between 0.98 and 0.7 s. A filter holder at the end of the reactor was used to collect the synthesized particles. Under these synthesis conditions, the synthesized products were always of the spinel crystal structure.

2.2. Reduction step

In order to improve the water-splitting performance and perhaps achieve reduction at lower temperatures, a small quantity of a carbon-containing species (activator) was mechanically mixed with the synthesized powders and the mixture was heated at about 800 °C in a laboratory reactor under Ar flow (Nalbandian et al., 2004). During heating in air the carbon-containing species is oxidized by O_2 from air. However, when the activator-containing solid is heated in an inert atmosphere without traces of oxygen, the carbon-containing species is decomposed by pulling away some of the redox reagents' lattice oxygen. This treatment ("activation") reduces the reagent and results in solids very active towards water splitting. Three different types of carbon containing species were employed: tylose, diesel fuel and wood chips. Compared to hydrogen or CO reductive means, these are low- or zero-cost waste streams of typically low organics concentration. The reduction process was not found sensitive to the activator type. The first set of experiments indicated that by adding less than 10 wt.% of reductant, reduction was not efficient and only very small quantities of hydrogen were produced; thus subsequent experiments reported below, were performed with 10 wt.% of reductant. Both "activated" and "non-activated" samples were comparatively evaluated.

2.3. Reagents characterization with respect to water-splitting

The materials tested were Mn/(Ni)–Zn–Fe–O systems of spinel ($Mn_x/(Ni)_xZn_{1-x}Fe_2O_4$) and of wustite ($Mn_x/(Ni)_xZn_yFe_{1-x-y}O$) structure as well as the component oxides Mn_3O_4, NiO, ZnO and Fe_2O_3. A special laboratory unit has been set-up for the evaluation of the redox reagents, described in detail in Nalbandian et al. (2004). The basic component of the unit is a U-shaped reactor placed in a temperature programmable furnace. All the materials were tested for the water splitting reaction by successive injections of water in a stream of Ar flowing continuously over the heated sample at temperatures ranging from 750 to 1100 °C. At preselected temperatures, known quantities of high purity water were injected to the reactor by using a microliter syringe. The effluent from the reactor was monitored through a mass spectrometer (MS) detector (Balzers, Omnistar). The sensitivity of the MS detector to hydrogen was calibrated by injecting a series of at least 10 constant volume loops of a 2 mol% H_2/Ar mixture. The quantities of unconverted water and of produced hydrogen were calculated, based on the areas of the corresponding MS injection peaks.

2.4. Regeneration under inert atmosphere

The most promising water splitting materials were studied by thermogravimetric analysis (TGA) in order to predict the effect of high temperature treatment to the reduction–oxidation cycles expected to occur under actual operating conditions. The temperature was ramped at 20 °C/min up to 800 °C, under Ar flow. After a 10 min period, the flow was switched to an O_2 mixture (5% O_2 in He) and an oxidation process took place for 60 min "saturating" the reagent with oxygen. The flow was switched again to Ar and the oxidized reagent was further heated (20 °C/min) up to 1300 °C, where it re-

mained for 30 min. During these heating and isothermal steps a weight loss was observed, attributed to reagents' reduction (O loss). The first cycle was completed by a cooling step at 20 °C/min back to 800 °C followed by a new introduction of the oxidizing mixture. During the second O_2 introduction, a weight gain was observed, attributed to re-oxidation of the material. The same steps were repeated twice in order to investigate the successive reduction–oxidation behaviour of the materials.

2.5. Set-up and testing of the thermochemical reactor/receiver

The main task of the intended test facility is the performance and monitoring of solar chemical hydrogen production by a two-step water splitting process with a redox system. The testing facility consists of a receiver-reactor as the central element capable of absorbing solar radiation provided by a solar furnace and at the same time of carrying out the necessary process steps at the required temperatures. The first step requires the supply of pure steam, for the oxygen releasing second step the supply of inert gas, i.e. nitrogen, is needed. The requirements with respect to high temperature operation of two alternating process steps under different conditions as well as the experience of reactor and receiver designing in former projects were taken into account during drafting, designing, and constructing the test facility finally leading to the reactor design depicted in Fig. 1.

Single-piece extruded multi-channel honeycombs to serve as catalyst carriers and cast parts to form the reactor's housing vessel (Fig. 1b) were manufactured from re-crystallized silicon carbide (reSiC) by STC Aps, Denmark. The honeycombs have dimensions ∅144 × 200 mm, high density of channels (90 cells per square inch, channel wall thickness 0.8 mm, cell size 2 × 2 mm, or 150 cells per square inch, channel wall thickness 0.6 mm, cell size 1.6 × 1.6 mm), porosity 36% and mean pore diameter 6 μm (measured by Hg porosimetry). The honeycombs are fixed in the centre of the reactor, which has a cylindrical symmetry (Fig. 1a). The focus of the so-

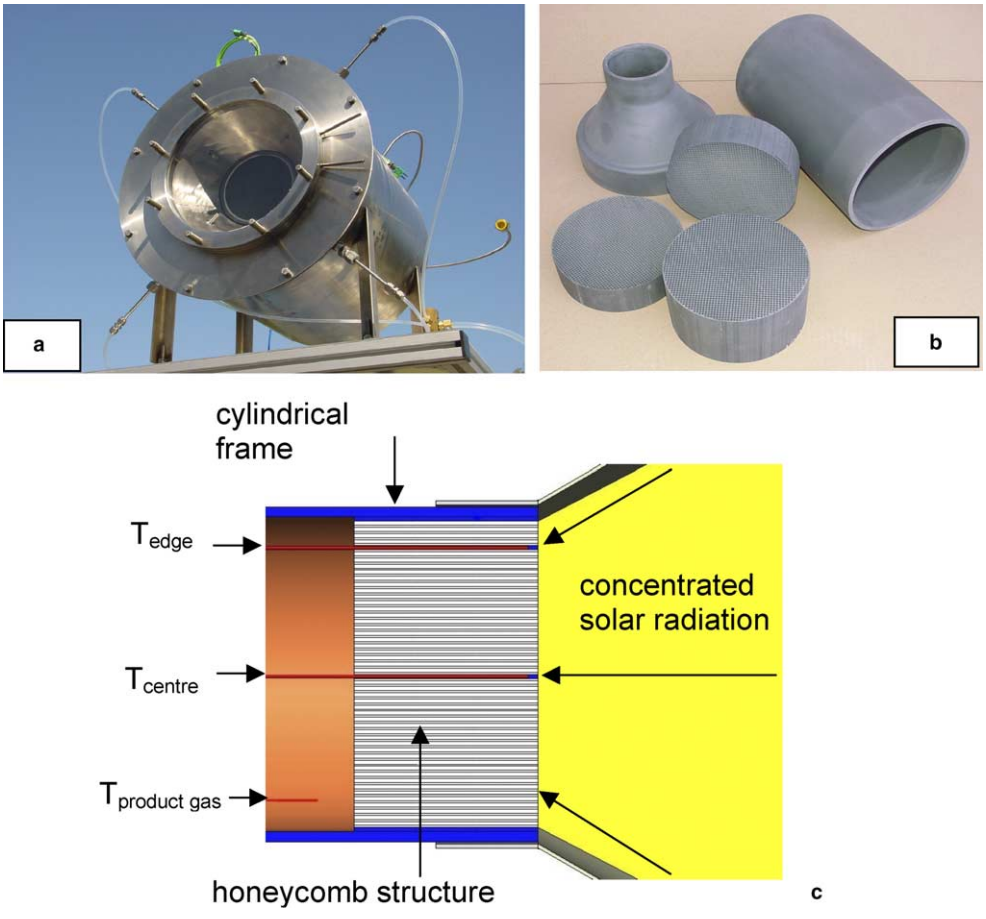

Fig. 1. (a) Front view of receiver-reactor for solar water splitting, (b) extruded reSiC honeycombs (carriers) and cast parts (housing vessel), (c) position of thermocouples in the absorber.

lar radiation concentrated by the solar furnace is located on the circular front area of the honeycombs, having a diameter of about 140 mm. The receiver is surrounded by isolating material and fixed in a cylindrical housing. The housing is slightly pressurised by a weak stream of nitrogen preventing condensation of water in the isolation material and emission of product gases. The front opening is sealed by a quartz window allowing the entrance of solar radiation and preventing the exit of process gas. The sealing can optionally be cooled by air or water. The process gases steam and nitrogen are fed into the reaction chamber using radial aligned stainless steel tubes and at the same time sucked by fans in the off-gas line to keep the pressure as close as possible to ambient conditions. A steam generator provides the necessary mass flow of 0–5 kg/h of steam at a temperature of about 150 °C. The steam can optionally be diluted by nitrogen at the same temperature. The reaction takes place in a ceramic honeycomb fixed in a ceramic cylinder whereas a ceramic funnel ensures the transfer of the product gases into an off-gas tube (Fig. 1b). The off-gas is cooled by mixing with nitrogen at ambient temperature and blown off after condensation of remaining steam. The reactor is integrated in a mini-plant including all necessary peripherals like inlet of feed gas, steam generator, cooling and treatment of the product gas, piping, devices for measurement of temperature, pressure, solar flux distribution, as well as a mass spectrometer for the detection of the produced hydrogen. The whole mini-plant is positioned and operated in the operational room of the solar furnace at DLR facilities, in Cologne, Germany. The temperature measurement was done by thermocouples within the reactor and on the surface of the housing. Two thermocouples were pushed into the channels of the honeycomb from the rear side (T_{centre} and T_{edge}) as indicated by Fig. 1(c) in order to monitor the absorber temperature. Potential falsification of measurement by direct radiation was avoided by clogging the two channels affected. Additionally for means of safety the front surface temperature of the quartz window was monitored by an infrared camera.

3. Results and discussion

3.1. Evaluation of redox material powders with respect to water-splitting

The results summarized below are presented in two types, either as ''total micromoles of hydrogen produced/g solid'' or as ''% mole conversion of injected water'' versus ''total micromoles of water injected/g solid''. Deactivation of all tested solids (decrease of conversion) was observed upon successive water injections. In order to keep a common basis, the conversions compared are the initial ones at 800 °C.

3.1.1. Initial activity—Materials tested without reduction

Appreciable H_2 yields on as-synthesized reagents (i.e without reduction) were obtained only from three material families, sintered MnZn-ferrites (SSS), some SHS Mn(Ni)–Zn–Fe–O products and ASP-synthesized ferrites. All other material families became active water splitters only after reduction (mixing with carbon containing species and heated to 800 °C under inert atmosphere).

- *MnZn-ferrites* (*SSS*): Samples having the chemical formula $(Mn_{0.75}Zn_{0.16}Fe^{2+}_{0.09})Fe^{3+}_2O_4$ sintered at 1250 °C under controlled O_2 pressure to ensure oxygen deficiency were active water splitters, producing pure hydrogen, however with very low conversions (60 μmoles of water injected over ~0.19 g of solid produced 0.6 μmoles of hydrogen i.e. conversion ≅ 1%). The activity of those samples is probably connected to their divalent iron content and since this was not high, the obtained H_2 yields are consequently small.
- *SHS products*: Two families of as-synthesized materials were distinguished: one of high and one of low conversion. Materials having the crystal structure of wustite $(A_{x'}B_{y'}Fe_{1-x'-y'})O$ exhibited high water splitting activity—a fact expected since they contain a significant amount of divalent iron. The water conversion of the ''best'' wustite-type materials reached 30% (60 μmoles of water injected over ~0.23 g of solid produced 18 μmoles of hydrogen). On the other hand, as-synthesized SHS materials having a spinel structure exhibited low conversions attributed to a very low divalent iron content achieved under the particular synthesis conditions. Further experiments are under way with different kinds and stoichiometries of dopant metals and less-oxygen-containing atmospheres in order to synthesize spinel phases with higher divalent iron content expected to perform better as water-splitters.
- *ASP products*: Spinel materials synthesized via ASP demonstrated significant water splitting activity and extremely high H_2 conversion ranging between 30% and 81% depending on the dopants stoichiometry (for the latter case, 60 μmoles of water injected over ~0.20 g of solid produced 48.6 μmoles of hydrogen). In addition, no CO_2 was observed in the product gases, indicating that these materials are prime candidates for water-splitting.

3.1.2. Materials tested after reduction

- *Iron oxides*: Two types of Fe_2O_3 were tested: commercial Fe_2O_3 (Merck Cat. No. 103924) (denoted as Fe_2O_3(B)), and an Fe_2O_3 spray-roasted from iron

chloride solutions (denoted as Fe_2O_3(A)). Maximum water conversion obtained was ≈35% (60 μmoles of water injected over ~0.19 g of solid produced 21 μmoles of hydrogen) with Fe_2O_3(A). Fe_2O_3(B) also had some considerable initial activity, however, much lower than Fe_2O_3(A) and deactivated very fast.

- *Dopant oxides*: NiO produced H_2, but at relatively low yields while Mn_3O_4 gave significant yields but was not considered as a strong candidate, because the produced H_2 was mixed with CO and CO_2 (coming from the organic-containing species not totally consumed during the reduction step).
- *NiZn ferrites* (*SSS*): As-synthesized materials showed negligible water conversion and H_2 production. However, after reduction, they gave appreciable activity to produce H_2 with conversions reaching 11% (60 μmoles of water injected over ~0.2 g of solid produced 6.6 μmoles of hydrogen).
- *MnZn-ferrites* (*SSS*): This family was capable for water splitting even without reduction (but with low conversion). After reduction, conversion reached ≅12% (60 μmoles of water injected over ~0.2 g of solid produced 7.2 μmoles of hydrogen).
- *SHS ferrites*: As already mentioned, as-synthesized MnZn-ferrites were inactive. After reduction the materials became water splitters, with initial conversion ≅7% (60 μmoles of water injected over ~0.19 g of solid produced 4.2 μmoles of hydrogen).

3.1.3. Final comparison of candidate water-splitting materials

A comparison among the materials tested with respect to the total hydrogen yield per gram of solid, is presented in Fig. 2 as a function of the total micromoles of H_2O injected (but in three separate plots for reasons of clarity). Table 1 presents the final comparison of the materials tested so far. In the first column the initial water conversion at 800 °C is presented, while the second column shows the total H_2 yield per gram of solid, for the first 1000 μmoles of injected water. The reduced Fe_2O_3(A) presents high initial conversion combined with relatively high H_2 yield. Similar results were obtained over the reduced SHS MnZn ferrites with somewhat lower initial conversion. The SHS-produced, wustite-type materials ($Mn_x/Ni_xZn_yFe_{1-x-y}O$) gave also high initial conversion and H_2 yields, without reduction. The reduced SSS MnZn spinel ferrites have also been proven active. The interesting fact is that spinels synthesized by ASP exhibited the highest conversions so far (30–81% depending on the dopants stoichiometry). An interesting comparison is between spinels of the stoichiometry $(Mn_{0.5}Zn_{0.5})Fe_2O_4$: these synthesized via SHS exhibited negligible conversion whereas those by ASP exhibited a conversion of 29.75%. The reasons for this discrepancy are currently under investigation; the superiority of ASP materials might be due to their much finer particle size compared to that of the SHS ones (250 nm versus 25 μm respectively). On the other hand the performance of the ASP-spinel materials further supports the arguments in the introduction that indeed, spinels can make use of the divalent metal ions for the splitting of water and the synthesis of hydrogen. All of the above materials are active water splitters; for identifying the "best" ones, regeneration capability should be also taken into account.

3.2. Evaluation of redox reagents with respect to regeneration capability

An effective redox pair water splitter has to be able for regeneration and H_2 production after repetitive reduction–oxidation cycles. Fig. 3 shows the weight and the temperature curves as a function of time for a sintered MnZn ferrite (synthesized via the SSS method), according to the procedure presented in Section 2. After the initial oxidation process at 800 °C where the sample gains weight, a weight loss of 0.68% is observed during heating under inert gas flow, in the temperature range 800–1300 °C, with maximum at 1075 °C. The same weight was gained back during the isothermal oxidation step at 800 °C. A second reduction cycle indicated very similar weight loss during heating, with maximum at 1090 °C.

Representative samples of all the important material families have been tested in the same way and the results are presented in Table 2. The temperature range within which each sample exhibited weight loss is reported. It is obvious that many tested materials can be reduced under inert atmospheres at temperatures well below 1300 °C and that the reduction–oxidation cycle can be repeated at least two times. Fe_2O_3 undergoes a highly repeatable weight loss-gain cycle, with a relatively high value of oxygen loss (3.5%); however exhibits the highestregeneration temperature (1285 °C). On the other hand, SHS-produced materials and sintered ferrites exhibit much lower regeneration temperatures, even though with less repeatability than Fe_2O_3. ASP $(Mn_{0.5}Zn_{0.5})Fe_2O_4$ exhibited an extremely high oxygen loss (11%) but at a relatively high regeneration temperature (1260 °C) whereas the ASP $ZnFe_2O_4$ showed the opposite trend: very low oxygen loss (1–2%) but at much lower temperature (1005 °C). All these families of materials seem most promising for further exploitation. It seems that a trade-off between oxygen regeneration percentage and regeneration temperature is necessary.

The results corroborate findings from previous literature (Tamaura et al., 1998b) where ferrites were claimed to exhibit relatively small amount of oxygen liberated during activation, but on the other hand lower, more workable operating temperatures. Taking into account

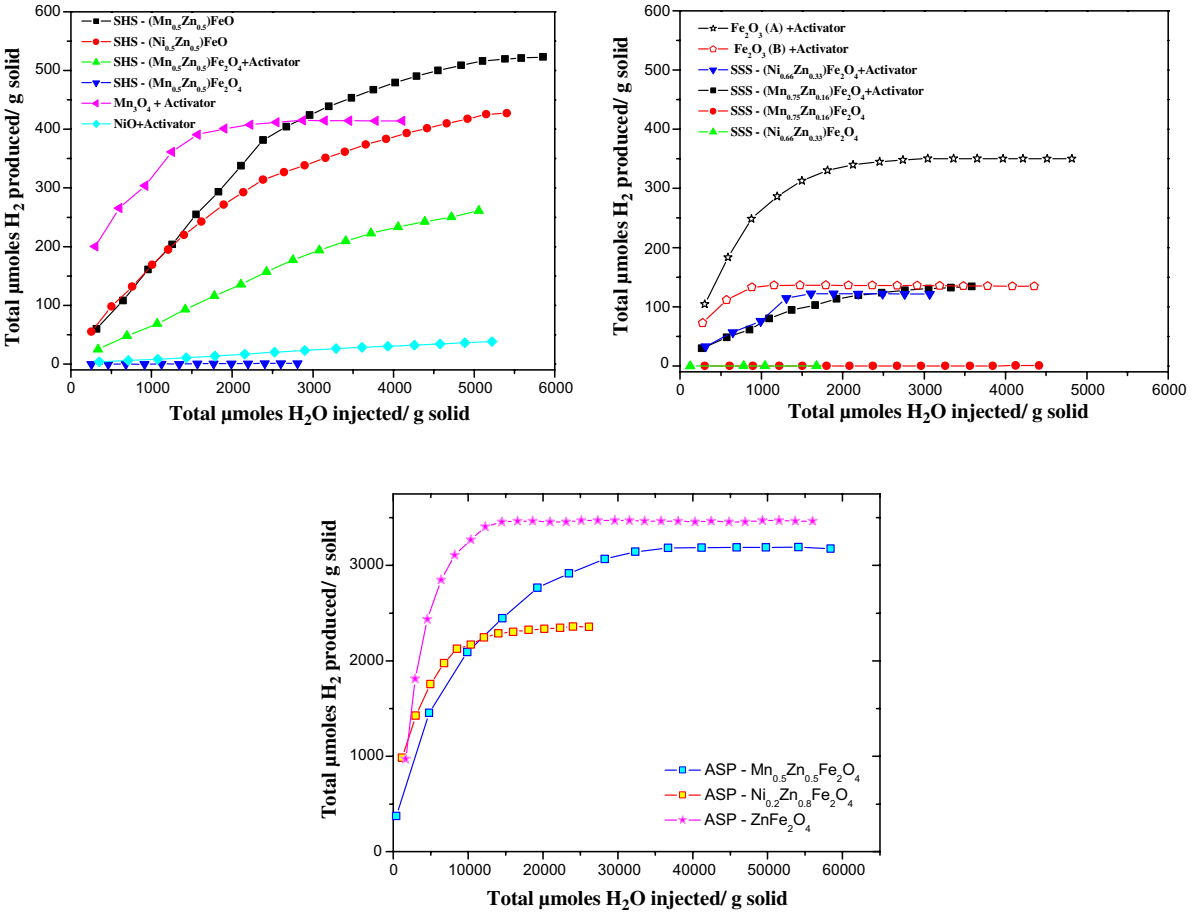

Fig. 2. Total micromoles of hydrogen produced/g solid versus total micromoles of water injected/g solid for representative samples.

the water splitting results mentioned before, the four families of materials presented in Table 2, seem the most promising for further exploitation.

3.3. Comparison with respect to maximum possible hydrogen yield

For a particular reagent composition the maximum possible H_2 yield can be calculated from the water splitting reaction stoichiometry and the maximum possible oxygen uptake from the water molecules. However, there was no way to know a priori, the maximum possible oxygen uptake capability in the reagents' lattice; therefore this quantity had to be determined implicitly. TGA was employed for this determination: by first reducing the reagent and then by keeping the reduced reagent under an oxidizing atmosphere for a prolonged period of time and measuring its weight gain until stabilization, one can measure the maximum amount of oxygen that this particular reagent composition is capable of uptaking. This quantity of oxygen can then be compared to the amount of oxygen actually uptaken from water (at a particular water splitting reaction temperature for example) in order to determine the reagents "water splitting efficiency". The respective procedure was as follows: reagent samples of 40–80 mg were heated with 20 °C/min up to 800 °C under Ar flow. After 10 min the flow was switched to an O_2 mixture (5% O_2 in He) and the oxidation process took place for 60 min, until no more weight gain of the sample was observed. In Fig. 4a such a TGA run for an SHS $(Mn_{0.5}Zn_{0.5})FeO$ material is shown. From the total weight gain (oxygen uptake in micromoles O_2/g solid) and the water splitting reaction ($H_2O \rightarrow H_2 + (1/2)O_2$) the maximum expected H_2 to be produced (in micromoles H_2/g solid) at the specific temperature (800 °C) can be calculated. At the laboratory water splitting unit ≈0.2 mg of the same material was heated at 800 °C, under Ar atmosphere. Water was injected at steady conditions, until the solid was almost completely deactivated. Fig. 4b shows the hydrogen yield expressed as "total micromoles H_2 produced/solid" as a function of "total

Table 1
Final comparison of the most representative materials tested with respect to water splitting

Material	Initial % mole conversion of injected H_2O (800 °C)	Total micromoles H_2 produced/g solid for 1000 μmoles H_2O injected/g solid (typically 0.2 g solid)
SHS $(Mn_{0.5}Zn_{0.5})FeO$	28 ± 3	200 ± 20
SHS $(Ni_{0.5}Zn_{0.5})FeO$	22 ± 3	170 ± 20
SHS $(Mn_{0.5}Zn_{0.5})Fe_2O_4$	0	0
ASP $(Mn_{0.5}Zn_{0.5})Fe_2O_4$	30 ± 3	297 ± 30
ASP $(Ni_{0.2}Zn_{0.8})Fe_2O_4$	80 ± 10	812 ± 50
ASP $ZnFe_2O_4$	65 ± 8	592 ± 40
SHS $(Mn_{0.5}Zn_{0.5})Fe_2O_4$ + activator	7.5 ± 2	65 ± 10
SSS $(Mn_{0.75}Zn_{0.16}Fe^{2+}_{0.09})Fe^{3+}_2O_4$	0.75 ± 0.2	4 ± 0.5
SSS $(Mn_{0.75}Zn_{0.16}Fe^{2+}_{0.09})Fe^{3+}_2O_4$ + activator	11 ± 2	80 ± 5
SSS $(Ni_{0.66}Zn_{0.33})Fe_2O_4$	0	0
SSS $(Ni_{0.66}Zn_{0.33})Fe_2O_4$ + activator	10.5 ± 2	80 ± 10
Fe_2O_3(A) + activator	34 ± 3	270 ± 20
Fe_2O_3(B) + activator	26 ± 3	135 ± 10
NiO + activator	1.1 ± 0.3	8 ± 1
Mn_3O_4 + activator[a]	66 ± 8	310 ± 20

Error ranges estimated from repetitive experiments.
[a] This material gave a small quantity of CO during the experiment.

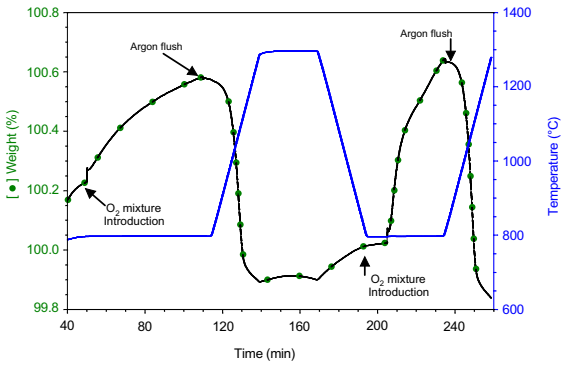

Fig. 3. Weight loss (—●—) and temperature (—) curves obtained during TGA study of a sintered SSS MnZn ferrite.

micromoles H_2O injected/g solid''. The total hydrogen yield obtained during the experiment was 1111 μmoles H_2/g solid, which is 90.8% of the maximum possible.

3.4. Set-up and testing of the thermochemical reactor/receiver

An experimental test campaign was carried out in the solar furnace to obtain experimental experience and to qualify the receiver–reactor with regard to the tasks of operating at temperatures up to 1200 °C and to carry out a thermochemical cycle for solar water splitting. The central aims of the test campaign were:

- test of feasibility of all components, in particular with regard to temperature resistance against thermal stress and temperature gradients,

Table 2
Regeneration comparison of the most representative materials tested

Material	Weight loss during first reduction (%)	Temperature range (°C)	Peak (°C)	Weight loss during second reduction (%)	Temperature range (°C)	Peak (°C)
SHS $(Mn_{0.5}Zn_{0.5})FeO$	1.59 ± 0.1	800–1250	1065	1.12 ± 0.1	800–1210	1060
SHS $(Mn_{0.5}Zn_{0.5})Fe_2O_4$	1.19 ± 0.1	800–1210	1045	0.79 ± 0.1	800–1210	1055
SSS MnZn ferrite	0.68 ± 0.1	800–1300	1075	0.79 ± 0.1	800–1210	1090
Fe_2O_3(A)	3.32 ± 0.2	1200–1300	1286	3.36 ± 0.2	1120–1295	1285
Fe_2O_3(B)	3.31 ± 0.2	1200–1300	1290	3.35 ± 0.2	1080–1300	1280
Fe_2O_3(A) + 10% activator	3.09 ± 0.2 (3.33 ± 0.2 based on Fe_2O_3(A))	1200–1300	1286	3.02 ± 0.2 (3.37 ± 0.2 based on Fe_2O_3(A))	1110–1295	1285
ASP $(Mn_{0.5}Zn_{0.5})Fe_2O_4$	10.90 ± 0.1	800–1270	1260	9.1 ± 0.1	800–1275	1280
ASP $ZnFe_2O_4$	1.20 ± 0.1	800–1285	1005	2.07 ± 0.1	800–1285	1095

Error ranges estimated from repetitive experiments.

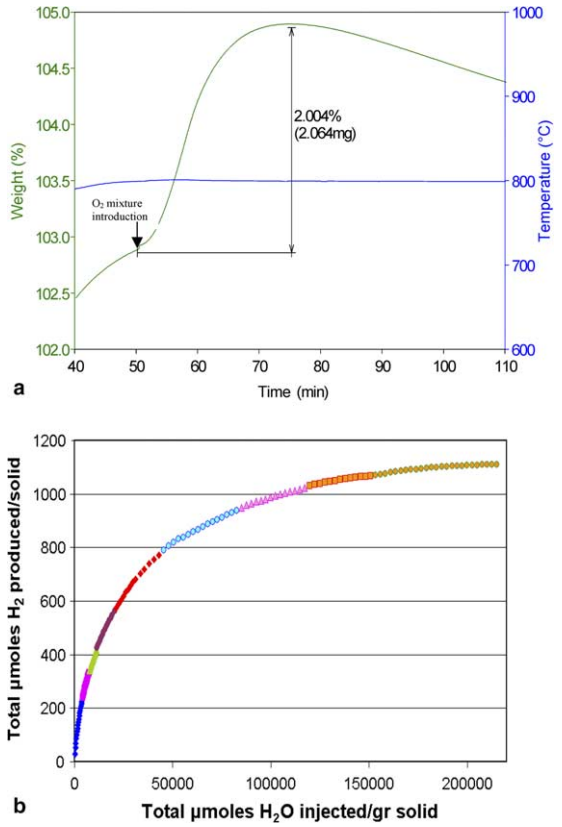

Fig. 4. SHS ($Mn_{0.5}Zn_{0.5}$)FeO material (a) TGA run, full oxidation, (b) hydrogen yield from water splitting at 800 °C.

- monitoring and enhancement of temperature profile within the absorber,
- influence of the solar flux distribution in the focus on the behaviour the absorber structure,
- study of influence of process parameters.

In a first series of tests the temperature distribution was monitored using different heating ramps and different levels of solar input power. The temperature of all components remained within the acceptable limits, even after many hours of operation. The only impact was observed at the surface of the radiation duct. Temperatures of up to 800 °C at this position caused discolorations—but without derogation of operation.

All components operated reliably even after several instantaneous jumps of input power, which can be a sudden start-up or shut down. A crucial point for the performance of the thermochemical cycle is the achievable temperature level and the temperature distribution within the absorber. In the first experiments the positions of the receiver aperture, which is the front face of the honeycomb absorber (see Fig. 1c), and the focal plane of the solar furnace almost coincided. As a result of that the temperature of the absorber near the irradiated face exhibited a strong gradient from 800 °C at the edge to 1250 °C in the centre. The gradient decreases within the absorber due to radial heat transfer. To reduce such a high gradient, the position of the aperture was shifted in axial direction causing a distance of 150 mm between aperture and focus position. This was done by shifting the reactor along the optical axis towards the concentrator of the solar furnace. By that the flux density in the aperture plane was equalised and the temperature difference was diminished to about 100 K near the front surface of the absorber and less within the honeycomb.

Fig. 5 shows the axial temperature profile in the honeycomb (length: 150 mm) after the modification described. The axial profile was determined by stepwise pulling the thermocouples to the rear part of the honeycomb. An almost constant temperature level—without considering the very first millimetres—could be achieved in the complete volume of the absorber after convergence to a thermal equilibrium. A further increase of that level is conceivable and intended for future. Therefore a maximum of volume and surface is potentially applicable for the thermochemical cycle, in particular for the regeneration step during the testing of coated honeycombs.

3.5. Transfer to a continuous operation

The operation of a commercial plant will require a continuous operation enabling a continuous supply of the main product hydrogen. At the same time each coated honeycomb will be available only about half of the time for hydrogen production because during the second half it is being regenerated. Nevertheless a continuous provision can be ensured by using a modular set-up of spatially fixed honeycomb absorbers in separate reaction chambers on a solar tower.

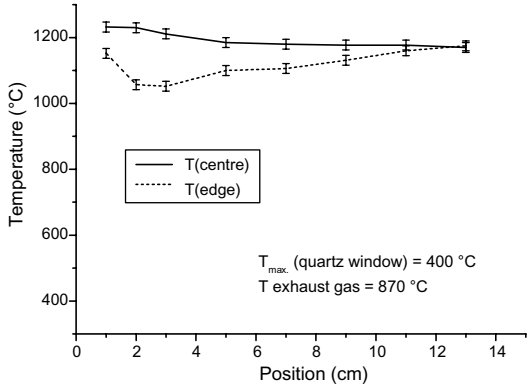

Fig. 5. Axial temperature distribution in the irradiated honeycomb (sealed reactor, near to thermal equilibrium, $error_{max}(T)$ = ±15 °C: resolution limit of data acquisition hardware).

One part of modules splits water while the rest is being regenerated. After completion of the reactions the regenerated modules are switched to the splitting process and vice versa by switching the feed gas. Simultaneous to that the solar flux will be optically varied in an alternating way depending on the status of the individual modules. This is necessary for the compensation of the different heat demands and different reaction temperatures in both reaction steps. When using ferrites the regeneration step is endothermic, the splitting step is slightly exothermic (Tamaura et al., 1998b) a fact that should decrease the hydrogen yield at higher temperatures, whereas the reaction rate is accelerated with increasing temperature level. The detailed effect of temperature on hydrogen yield and the optimisation of the water splitting temperature reaction is the subject of current on-going work. It is certain however, that this would be below the regeneration temperature of most of the materials tested (1200–1300 °C). Therefore an operation at alternating temperature levels will presumably be necessary. Based on the powder experiments and on the available reaction volume the duration of a single cycle is estimated as considerably less than 1 h. Therefore several cycles will be operated at one day.

Experimental values of the energy conversion efficiency, i.e. the ratio of the energy stored in chemical form (enthalpy change × chemical conversion), to the solar energy input to the reactor are not yet available due to the fact that within the scope of this work, only non-solar experiments of water splitting by the redox materials as powders have been performed and reported. The potential efficiency of the process in the solar test reactor depends in one hand on the conversion of water to hydrogen achieved and in the other hand on the thermal losses of the solar reactor. It should be borne in mind that currently both these factors are not optimised. The thermal qualification of the solar test reactor provided mean thermal losses of about 2.3 kW during water splitting and of about 5.1 kW during regeneration under steady state conditions. About 1/3 of that amount may be recoverable because it is excess heat of the product gases. With the conversion achieved so far (≈81%) and a projected mass flow rate of steam in the solar reactor about 1 kg/h, preliminary calculations based on Tamaura's thermodynamic data (Tamaura et al., 1998b) have shown that the efficiency of the solar test reactor (lower heating value of hydrogen produced/solar energy input) can reach up to 55%. The efficiency will be optimised by the development of enhanced water-splitting compositions with higher water-to-hydrogen conversion, by thermally optimising the reactor and in particular by the scale-up of the process, which reduces the ratio of surface of the reactor to the reactive zone and thereby the heat losses. A decrease of the overall efficiency will occur due to the energy required to recycle/separate the inert gas (such as nitrogen) needed to provide inert atmosphere for the reduction step. Depending on the size of the plant, pressure swing absorption or membrane methods will be applied to separate the released oxygen and to purify the nitrogen, methods needing about 0.25 kW h/Nm^3 nitrogen. The exact value depends on the required purity of the nitrogen, which is still an object of investigation. Preliminary calculations indicate that, in general, a reduction of efficiency of about one fourth is expected by the need to use pure nitrogen as flushing gas. This reduction can be counterbalanced as mentioned above, by improvements in the overall reactor design and operation that can maximize hydrogen production during the water-splitting step and minimize heat losses during entire continuous operation. However, a recent investigation (Takahashi et al., 2004) shows a release of oxygen in similar redox systems that can reach nearly 100% under air-flow conditions. This opens the perspective to avoid inert gas completely or at least minimise the required amount.

4. Conclusions

A new promising method for performing solar heated thermo-chemical process applying two-step water splitting operating at a moderate temperature level of about 800–1200 °C has been presented. It includes the combination of a support structure capable of achieving high temperatures when heated by concentrated solar radiation, with an iron-oxide-based redox system suitable for the performance of water dissociation and subsequent regeneration at these temperatures. To the authors' knowledge this is the first time that such a solar reactor concept based on monolithic honeycombs is being proposed and tested.

A wide variety of iron-oxide-based redox pair systems was synthesized, characterized and comparatively evaluated with respect to water splitting and regeneration capability. The proposed concept has been proved: the synthesized catalyst systems are able to split water and generate hydrogen as the only product, at temperatures as low as 800 °C with conversions reaching 80% in terms of water (amount of water converted/total amount of water). From the regeneration experiments, it became obvious that several of these materials could be reduced under inert atmospheres at temperatures well below 1300 °C and that the reduction–oxidation cycle could be repeated at least two times, indicating high potential for their integration in a two-step water splitting process within a solar system. Hydrogen yields more than 90% of the maximum possible were achieved from at least one catalyst system synthesized.

A dedicated solar chemical receiver/reactor suitable to carry out the described two-step thermo-chemical cycle has been designed, constructed, and qualified. A test programme has been developed. The temperature profile

within the ($\varnothing 144 \times 200$ mm) honeycombs has been homogenised to minimise temperature gradients and provide almost equal reaction conditions within the whole volume of the honeycomb absorber, being now capable of achieving uniform temperatures of the order of 1300 °C.

The next steps of the work include on one hand further optimisation of the redox materials with respect to dopants stoichiometry in order to further improve their hydrogen yield and their capability for regeneration and on the other hand cyclic testing of both process steps using redox reagents-coated honeycombs incorporated in the solar reactor.

Acknowledgments

The work has been funded by the European Commission within the Project "Catalytic monolith reactor for Hydrogen generation from solar water splitting-HYDROSOL" (ENK6-CT-2002-00629), under the 'Energy, environment and sustainable development (part b: Energy)' Programme (1998–2002).

References

Agrafiotis, C., Zaspalis, V.T., 2004. Self-propagating high-temperature synthesis of MnZn-ferrites for inductor applications. Journal of Magnetism and Magnetic Materials 283 (2–3), 364–374.

Ehrensberger, K., Frei, A., Kuhn, P., Oswald, H.R., Hug, P., 1995. Comparative experimental investigations of the water-splitting reaction with iron oxide $Fe_{1-y}O$ and iron manganese oxides $(Fe_{1-x}Mn_x)_{1-y}O$. Solid State Ionics 78, 151–160.

Ehrensberger, K., Kuhn, P., Shklover, V., Oswald, H.R., 1996. Temporary phase segregation processes during the oxidation of $(Fe_{0.7}Mn_{0.3})_{0.99}O$ in N_2–H_2O atmosphere. Solid State Ionics 90, 75–81.

Fend, T., Hoffschmidt, B., Pitz-Paal, R., Reutter, O., Rietbrock, P., 2004. Porous materials as open volumetric solar receivers: experimental determination of thermophysical and heat transfer properties. Energy 29 (5–6), 823–833.

Heck, R.M., Farrauto, R.J., 1995. Catalytic air pollution control—commercial technology. Van Nostrand Reinhold, New York, USA.

Hoffschmidt, B., Fernández, V., Konstandopoulos, A.G., Mavroidis, I., Romero, M., Stobbe, P., Téllez, F., 2001. Development of ceramic volumetric receiver technology, In: Funken, K.-H., Bucher, W. (Eds.), Proceedings of 5th Cologne Solar Symposium, June 21, Forschungsbericht 2001-10, DLR, Germany, pp. 51–61.

Kaneko, H., Hosokawa, Y., Gokon, N., Kojima, N., Hasegawa, N., Kitamura, M., Tamaura, Y., 2001. Enhancement of O_2-releasing step with Fe_2O_3 in the water splitting by $MnFe_2O_4$–Na_2CO_3 system. Journal of Physics and Chemistry of Solids 62, 1341–1347.

Kaneko, H., Kojima, N., Hasegawa, N., Inoue, M., Uehara, R., Gokon, N., Tamaura, Y., Sano, T., 2002a. Reaction mechanism of H_2 generation for H_2O/Zn/Fe_3O_4. International Journal of Hydrogen Energy 27, 1023–1028.

Kaneko, H., Ochiai, Y., Shimizu, K., Hokokawa, Y., Gokon, N., Tamaura, Y., 2002b. Thermodynamic study based on the phase diagram of the Na_2O–MnO–Fe_2O_3 system for H_2 production in three-step water splitting with Na_2CO_3/$MnFe_2O_4$/Fe_2O_3. Solar Energy 72, 377–383.

Kaneko, H., Kodama, T., Gokon, N., Tamaura, Y., Lovegrove, K., Luzzi, A., 2004. Decomposition of Zn-ferrite for O_2 generation by concentrated solar radiation. Solar Energy 76, 317–322.

Kodama, T., 2003. High-temperature solar chemistry for converting solar heat to chemical fuels. Progress in Energy and Combustion Science 29 (6), 567–597.

Kodama, T., Kondoh, Y., Kiyama, A., Shimizu, K. 2003. Hydrogen production by solar thermochemical water-splitting/methane-reforming process. In: Proceedings of International Solar Energy Conference ISEC Hawaii, USA, 16–18 March 2003, pp. 121–128.

Kogan, A., 2000. Direct solar thermal splitting of water and on-site separation of the products-IV. Development of porous ceramic membranes for a solar thermal water-splitting reactor. International Journal of Hydrogen Energy 25, 1043–1050.

Kojima, M., Sano, T., Wada, Y., Yamamoto, T., Tsuji, M., Tamaura, Y., 1996. Thermochemical decomposition of H_2O to H_2 on cation-excess ferrite. Journal of Physics and Chemistry of Solids 57 (11), 1757–1763.

Konstandopoulos, A.G., Kostoglou M., Skaperdas, E., Papaioannou, E., Zarvalis, D., Kladopoulou, E., 2000. Fundamental studies of diesel particulate filters: transient loading, regeneration and aging, SAE Trans. 109 (J. Fuels and Lubricants) Paper SAE Tech. Paper 2000-01-1016. Also in Diesel Exhaust Aftertreatment 2000, SAE SP-1497 pp. 189–211.

Konstandopoulos, A.G., Papaioannou, E., Zarvalis, D., Skopa, S., Baltzopoulou, P., Kladopoulou, E., Kostoglou, M., Lorentzou, S., 2005. Catalytic filter systems with direct and indirect soot oxidation activity, SAE Tech. Paper 2005-01-0670 (SP-1942).

Lorentzou, S., Karadimitra K., Agrafiotis C., Konstandopoulos A.G., 2004. New routes for ferrite powders synthesis. In: PARTEC 2004, International Conference for Particle Technology, Nuremberg, Germany, 16–18 March.

Nalbandian, L., Zaspalis, V.T., Evdou, A., Agrafiotis, C., Konstandopoulos, A.G., 2004. Redox materials for hydrogen production from the water decomposition reaction. Chemical Engineering Transactions 4, 43–48.

Palumbo, R., Keunecke, M., Möller, S., Steinfeld, A., 2004. Reflections on the design of solar thermal chemical reactors: thoughts in transformation. Energy 29 (5–6), 727–744.

Perkins, C., Weimer, A.W., 2004. Likely near-term solar-thermal water splitting technologies. International Journal of Hydrogen Energy 29 (15), 1587–1599.

Rubbia, C., 2003. Hydrogen at crossroads between science and politics. Conference on the Hydrogen Economy—A Bridge to Sustainable Energy, Brussels, 16–17 June.

Steinfeld, A., Kuhn, P., Reller, A., Palumbo, R., Murray, J., Tamaura, Y., 1998. Solar-processed metals as clean energy carriers and water-splitters. International Journal of Hydrogen Energy 23 (9), 767–774.

Steinfeld, A., Sanders, S., Palumbo, R., 1999. Design aspects of solar thermochemical engineering—A case study: Two-step water-splitting cycle using the Fe_3O_4/FeO redox system. Solar Energy 65 (1), 43–53.

Steinfeld, A., 2002. Solar hydrogen production via a two-step water-splitting thermochemical cycle based on Zn/ZnO redox reactions. International Journal of Hydrogen Energy 27, 611–619.

Steinfeld, A., 2005. Solar thermochemical production of hydrogen—a review. Solar Energy 78, 603–615.

Sturzenegger, M., Nuesch, P., 1999. Efficiency analysis for a manganese-oxide-based thermochemical cycle. Energy 24, 959–970.

Takahashi, Y., Aoki, H., Kaneko, H., Hasegawa, N., Suzuki, A., Tamaura, Y., 2004. Oxygen-gas-releasing reaction of Zn ferrite by Xe lamp beam irradiation in air at 1800 K. Solid State Ionics 172, 89–91.

Tamaura, Y., Steinfeld, A., Kuhn, P., Ehrensberger, K., 1995. Production of solar hydrogen by a novel, 2-step, water-splitting thermochemical cycle. Energy 20 (4), 325–330.

Tamaura, Y., Hasegawa, N., Kojima, M., Ueda, Y., Amano, H., Tsuji, M., 1998a. Water splitting with the Mn(II)-Ferrite CaO–H_2O system at 1273 K. Energy 23 (10), 879–886.

Tamaura, Y., Kojima, M., Sano, T., Ueda, Y., Hasegawa, N., Tsuji, M., 1998b. Thermodynamic evaluation of water splitting by a cation excessive (Ni, Mn) Ferrite. International Journal of Hydrogen Energy 23, 1185–1191.

Tamaura, Y., Ueda, Y., Matsunami, J., Hasegawa, N., Nezuka, M., Sano, T., Tsuji, M., 1999. Solar hydrogen production by using ferrites. Solar Energy 65 (1), 55–57.

Tamaura, Y., Kojima, N., Hasegawa, N., Inoue, M., Uehara, R., Gokon, N., Kaneko, H., 2001. Stoichiometric studies of H_2 generation reaction for H_2O/Zn/Fe_3O_4 system. International Journal of Hydrogen Energy 26, 917–922.

Trovarelli, A., 1996. Catalytic properties of ceria and CeO_2-containing materials. Catalysis Reviews in Science and Engineering 38, 439–520.

Tsakaloudi, V., Papazoglou, E., Zaspalis, V.T., 2004. Microwave firing of MnZn-ferrites. Materials Science and Engineering B 106 (3), 289–294.

Weidenkaff, A., Nüesch, P., Wokaun, A., Reller, A., 1997. Mechanistic studies of the water-splitting reaction for producing solar hydrogen. Solid State Ionics 101–103 (2), 915–922.